Available online at www.elixirpublishers.com (Elixir International Journal)

Nanocomposite Materials

Elixir Nanocomposite Materials 50 (2012) 10624-10627

ISSN: 2229-712X

Synthesis and electrical properties of PbS_xO_{1-x} Nanocomposites

S. Rajasekar[a], S. Tamilselvan[b], R. Jeyasekaran[c], M. Gulam Mohamed[d], P.Marimuthu[a], I.Vetha Potheher[e] and M. Vimalan[f*]

[a]Syed Ammal Engineering College, Ramanathapuram, India.

[b]Department of Physics, Arignar Anna Government Arts College, Cheyyar, India.

[c]Department of Physics, Saveetha Engineering College, Chennai, India.

[d]Department of Physics, The New College, Chennai, Tamilnadu, India.

[e]Department of Physics, Anna University, Thiruchirapalli, Tamilnadu, India.

[f,*]Physics Research Centre, S.T. Hindu College, Nagercoil, Tamil Nadu, India.

ARTICLE INFO

Article history:

Received: 1 August 2012;

Received in revised form:

31 August 2012;

Accepted: 20 September 2012;

Keywords

Composites,

Semiconductors,

X-ray diffraction,

Electrical properties.

ABSTRACT

PbS_xO_{1-x} (x = 0.0, 0.2, 0.4, 0.5, 0.6, 0.8 and 1.0) nanocomposites were prepared by the microwave assisted solvothermal method using a domestic microwave oven for the first time. The yield percentage and the preparation time were noted. The samples were annealed at 200 ^oC for 1 hr to improve the ordering. Grain sizes and lattice parameters were determined by carrying out X-ray powder diffraction measurements. AC and DC electrical measurements were carried out on palletised samples at various temperatures ranging from 40-150 ^oC. Results of the present study reveal that the space charge contribution plays a significant role in the charge transport process and polarizability in all the seven nanocrystals studied. The electrical parameters increase with increasing temperature. Results of the present study reveal that the space charge contribution plays a significant role in the charge transport process and polarizability in all the seven nanocrystals studied.

Introduction

The nanoparticles possess a variety of properties depending on their chemical composition. Development of nanotechnologies in the recent decades has led to the widespread use of nanomaterials in all kinds of common industrial and medical applications [1-2]. Nanomaterials have broad applications in a variety of fields because of their unusual and size dependent optical, magnetic, electronic and chemical properties [3, 4]. The semiconductor nanoparticles belong to the state of matter in transition between molecules and bulk solids in which the relevant physical dimensions changes on the length of a few to a few hundred nanometers. For over a decade, II-VI semiconductors have attracted growing interest owing to their possible application in optoelectronics. There are generally recognized eight II-VI semiconductor materials. They are: ZnO, ZnS, ZnSe, ZnTe, CdO, CdS, CdSe, and CdTe. The electronic and optical properties of II-VI compound semiconductor nanoparticles have been extensively investigated in view of a wide variety of applications [5]. With change in the particle size, dramatic modifications of their electronic and optical properties takes place due to the three-dimensional quantum confinement of electrons and holes when the size of the particle approaches the Bohr radius of an exciton [6,7]. In addition to the change in electronic and optical properties, the structural behavior also exhibits changes with change in particle size. In this case, several researchers have got interested in the doped and co-doped semiconductor nanocrystals, semiconductor- dielectric nanocomposites, semiconductor-polymer nanocomposites, two-component nanocomposites, etc [8]. Several research reports are available on pure and doped individual nanoparticles of PbS and PbO [9-11]. To our knowledge, no data concerning AC and DC conductivity are available in literature. In the present work, we report the synthesis of magnesium doped PB S_xO_{1-x} nanoparticles by simple solvothermal methods using domestic microwave oven, for the first time. The prepared samples were characterized by carring out X-ray powder diffraction (PXRD) and electrical (DC and AC) mesurements. The results obtained are reported and disucssed here in this paper.

Experimental

Analytical reagent (AR) grade Lead acetate and urea or thiourea in 1:3 molecular ratio were mixed and dissolved in ethylene glycol and kept in a domestic microwave oven. Microwave (2.45 GHz) iiradiation was carried out till the solvent (ethylene glycol) was evaporated completely. The colloidal precipitate obtained was cooled, washed several times with distilled water and acetone to remove the organic impurities present, if any. The washed samples were then dried in atmospheric air and collected as the yield (Table 1). The reactions were found to be (within 38 min) and highly yielding.

A total of seven samples were prepared with x having the values 0.0 (PbO), 0.2, 0.4, 0.5, 0.6, 0.8 and 1.0 (PbS). The samples were annealed at 200 ^oC for 1 hr to improve the ordering. Characterization studies were made on the annealed samples.

The mass of the product nanocrystals was measured accurately and used for the estimation of yield percentage. The yield percentage was obtained by using the relation

$$Yield\ Percentage = \frac{Mass\ of\ the\ Product}{Sum\ of\ the\ Masses\ of\ the\ Reactants} X100$$

The reactions were found to be (within 33 min) and highly yielding.

An automated X-ray powder diffraction (PXRD) data were obtained with a PANalytical diffractometer equipped with CuK_α radiation (λ = 1.54056Å). The PXRD patterns were compared

Tele:

E-mail addresses:

with the help of JCPDS files. The grain sizes were determined by using the Scherrer formula [12].

$$D = \frac{k\lambda}{\beta\, Cos\theta}$$

Where D is the mean diameter (size) of the grains, k (=0.9) is the size factor, β is the full width at half maximum (in radians), λ is the wavelength of the X-radiation used and 2θ is the angle at which the maximum intensity was observed. Five to six diffraction peaks were chosen wherever possible and consistency in the grain sizes obtained from using their width was confirmed. The values obtained are provided in Table 1.

All the seven nanocrystalline samples prepared were pelletised (although agglomeration of particles is possible) using a hydraulic press (with a pressure of about 4 tons only in order to reduce the agglomeration of particles) and used for the electrical measurements. The flat surfaces of the cylindrical pellets were coated with good quality graphite to obtain a good conductive surface layer. A traveling microscope (Least count = 0.001 cm) was used to measure the dimensions of the pellets.

The DC electrical conductivity measurements were carried out (within an accuracy of ±3%) for the pellets of all the seven samples prepared in the present study using the conventional two-probe technique using a million megohmmeter at various temperatures ranging from 40-150°C in a way similar to that followed by Mahadevan and his co-workers [13-14]. Temperature was controlled to an accuracy of ±1°C. The observations were made while cooling the sample. The DC electrical conductivity (σ_{dc}) of the pellet was calculated using the relation

$$\sigma_{dc} = {}^{d}/_{RA},$$

where R is the measured resistance, d is the thickness of the pellet and A is the area of the flat face of the pellet in contact with the electrode.

The dielectric measurements were carried out (within an accuracy of ±2%) for the pellets of all the seven samples prepared in the present study using the conventional parallel plate capacitor method using an LCR meter (Agilent 4284A) with a fixed frequency of 1 kHz in a way similar to that followed by Mahadevan and his co-workers [13-15]. Capacitance (C_c) and dielectric loss factor (tanδ) were measured at various temperatures (controlled to an accuracy of ±1°C) ranging from 40-150°C while cooling the sample. Air capacitance (C_a) was also measured for the thickness equal to that of the pellet. The area of the pellet in contact with the electrode is same as that of the electrode. Since the variation of air capacitance with temperature was found to be negligible, air capacitance was measured only at room temperature. The dielectric constant of the pellet was calculated using the relation

$$\epsilon_r = {}^{C_c}/_{C_a}$$

The AC electrical conductivity (σ_{ac}) was calculated using the relation

$$\sigma_{ac} = \epsilon_0 \epsilon_r \omega \tan\delta$$

where, ϵ_0 is the permittivity of free space (8.85 x 10^{-12} C^2N^{-1} m^{-2}) and ω is the angular frequency ($\omega \approx 2\pi f$; f is the frequency).

Results and Discussion

The yield percentage is observed to be significantly high for all the samples prepared. The yield percentage, reaction time and grain size observed in the present study are provided in Table. 1. The PXRD patterns observed for PbS and PbO compare well with that available in the literature [9-11] indicating that the materials of the samples prepared in the present study are basically PbS and PbO. The changes in PXRD patterns observed for the nano composites with those of end members indicate that they are mixed ones. Fig. 1 shows the PXRD pattern of the $PbS_{0.5}O_{0.5}$ nanocrystal.

In the diffraction patterns, peak broadening is due to four factors: micro strain (deformation of the lattice), crystalline faults (extended defects), crystalline domain size, and domain size distribution. The two main properties extracted from peak width analysis are the crystallite size and lattice strain. Crystallite size is a measure of the size of coherently diffracting domain. X-ray line broadening is used for the investigation of dislocation distribution. The Bragg peak is affected by Crystallite size and lattice strain in different ways. Both these effects increase the peak width, the intensity of the peak and shift the 2θ peak position accordingly.

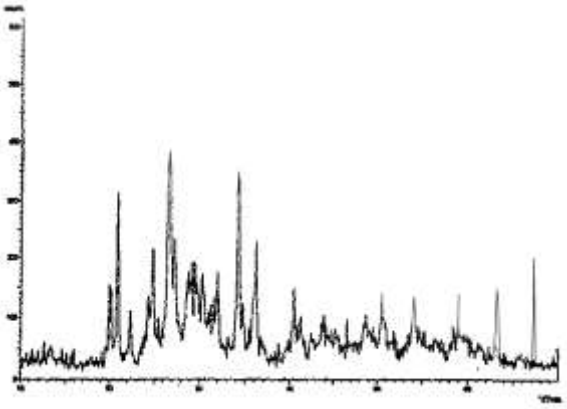

Fig. 1. The PXRD pattern for $PbS_{0.5}O_{0.5}$ nanocrystals

The Bragg width contribution from crystallite size is inversely proportional to the crystallite size. Although X-ray profile analysis is an average method, they still hold an unavoidable position for grain size determination [16]. If we assume that the analyzed PbS_xO_{1-x} nanocrystals are without free strain and crystalline faults, the peak broadening will only be due to the domain size that can be calculated from the full width at half maximum (FWHM) intensity of PbS_xO_{1-x} nanocomposites, according to the Scherrer equation. The values obtained are provided in Table 1. Clearly it is evident that the crystallite growth in PbS_xO_{1-x} has become smaller with the increase of 'x', and particularly when x = 0.5 and 0.6 smaller sizes have been achieved.

The dielectric parameters, viz. ε_r, tan δ, σ_{ac} and σ_{dc} observed in the present study are shown in Figs. 2-5. The ε_r values obtained for the end members (3.131 for PbS and 4.485 for PbO) are very small. All the four electrical parameters increase with the increase in temperature for all the seven PbS_xO_{1-x} nanocrystals considered in the present study. In the case of PbS_xO_{1-x} nanocrystals, there is no systematic variation of ε_r ,tan δ, σ_{ac} and σ_{dc} values with respect to the composition. However, all the four values are found to be more for PbO nanocrystals. The ε_r value at all temperatures considered for all the systems, it decreases the ε_r value. The ε_r are decreased by the urea addition in the case of systems with x = 0.0 to 1.0. This trend is found to be nearly true with the σ_{ac} values. However, in all the systems, it is found that the urea addition increases the temperature coefficient of σ_{dc} very significantly. The above

results indicate that urea addition creates more thermal defects to increase the DC conductivity when the temperature is increased.

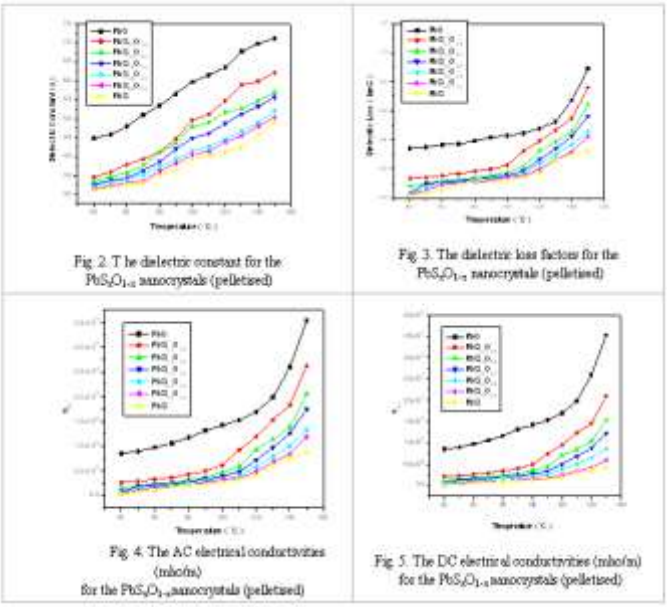

Fig. 2. The dielectric constant for the PbS_xO_{1-x} nanocrystals (pelletised)

Fig. 3. The dielectric loss factors for the PbS_xO_{1-x} nanocrystals (pelletised)

Fig. 4. The AC electrical conductivities (mho/m) for the PbS_xO_{1-x} nanocrystals (pelletised)

Fig. 5. The DC electrical conductivities (mho/m) for the PbS_xO_{1-x} nanocrystals (pelletised)

In semiconductors a fundamental optical absorption process may occur if the photon energy is larger than the band gap thus creating an electron and a hole. This electron hole (e-h) pair can move independently of one another resulting in electrical conductivity. The separation of the electron and the hole usually is large enough so that there is no coulombic attraction between them. Such description of non-interacting electrons and holes corresponds to the so called single particle presentation. If the absorption occurs at point (k =0) and with a photon energy slightly below the band gap, electrons and holes do interact via coulomb potential and form quasiparticle that corresponds to a hydrogen-like bound state of an e-h pair which is referred to as an exciton.

In conventional semiconductors the excitons are classified as weakly bound Mott-Wannier excitons, for which the e-h distance is large in comparison with the lattice constant, while a strongly bound Frenkel exciton with an e-h distance comparable to the lattice constant occurs in ionic or rare gas crystals and in organic materials. The Wannier exciton resembles a hydrogen atom. Therefore, similarly to the hydrogen atom, this exciton is characterized by the exciton Bohr radius (a_B)

$$a_B = \frac{h^2 \epsilon_r}{4\pi^2 e^2}\left(\frac{1}{m_e} + \frac{1}{m_h}\right)$$

where ε_r is the dielectric constant, and m_e and m_h are the effective masses of electron and hole respectively, e is the electronic charge and h is the Planck's constant.

The effective e-h mass is smaller than the electron mass m_e, and the dielectric constant is several times larger than 1. This is why the exciton Bohr radius is significantly larger and the exciton Rydberg energy (R^*_y), $R^*_y = e^2/2\ \varepsilon_r\ a_B$ is significantly smaller than the relevant values of the hydrogen atom. Absolute values of a_B for the common semiconductors range in the interval 1-10 nm and the exciton Rydberg energy takes values of approximately 1-100 meV [17].

The binding energy of the exciton is strongly influenced by the presence of other electrons in the solid which screen the hole. In a continuum approximation the screening can be described by the dielectric constant of the material. The binding energies of the exciton are generally very small (large excitonic radius), i.e. they are on the scale of a few meV [18]. The excitonic states in solids are experimentally observable only at low temperatures because of the dissociation of the exciton into free carriers by the available thermal energy at room temperature. In contrast, in case of molecules the e-h pair is localized at the molecule resulting in a strong coulomb interaction. Thus, there is very little screening which leads to a strong excitonic absorption.

Nanoparticles lie between the infinite solid state and molecules. When one reduces the dimension of the solid to a nanometer size (i.e. to a nanoparticle) the size of the exciton becomes comparable or even larger than the particle. This results in the splitting of the energy bands into discrete quantization levels, and the band gap starts opening. This is called the size quantization effect.

The electrical resistivity of nanocrystalline material is higher than that of both conventional coarse grained polycrystalline material and alloys. The magnitude of electrical resistivity and hence the conductivity in composites can be changed by altering the size of the electrically conducting component. The σ_{dc} and σ_{ac} values observed in the present study are very small (i.e. the resistivities are very large). When the crystal (grain) size is smaller than the electron mean free path, grain boundary scattering dominates and hence electrical resistivity is increased.

The low value observed for ε_r indicates that the polarization mechanism in the nanocrystals considered is mainly due to the space charge polarization. So, it can be understood that there seems the occurrence of nano-confined states in the case of all the seven systems (Table 1) considered in the present study which may substantially contribute to the electrical properties. Thus, the space charge contribution plays an important role in charge transport process and polarizability in the case of almost all the seven systems considered in the present study.

Conclusion

PbS_xO_{1-x} composite nanocrystals were prepared via a convenient microwave assisted solvothermal method using domestic microwave oven and characterized by PXRD and electrical measurements. The yield percentage and grain size obtained indicate that the preparation method used in the present study is a reasonable one for the preparation of PbS_xO_{1-x} composite nanocrystals. The electrical parameters observed increase with the increase in temperature and indicate that all the seven nanocrystals prepared are semiconductors. Results obtained in the present study indicate that there seems the occurrence of nano-confined states in the case of all the seven systems studied which may substantially contribute to the electrical properties. Hence, it is clearly understood that the space charge contribution plays an important role in the charge transport process and polarizability in the case of almost all the systems considered in the present study.

Reference

[1] K. Muraia, Y. Watanabe, Journal of Ceramic Processing Research 8 (2007) 114.

[2] A. Dhawan, V. Sharma, and D. Parmar, "Nanomaterials: a challenge for toxicologists," Nanotoxicology 3 No. 1 (2009) 1.

[3] K. Muraia, Y. Watanabe et al Journal of Ceramic Processing Research. 8 (2007) 114.

[4] R. J. Aitken, M. Q. Chaudhry, A. B. A. Boxall, and M. Hull,"Manufacture and use of nanomaterials: current status in the K and global trends," Occupational Medicine 56 (2006) 300.

[5] V. Sivasubramanian, A. K. Arora, M. Premila, C. S. Sundar and V. S. Sastry, Physica E31 (2006) 93.

[6] R. J Bandaranayke, G. W. Wen, J. Y. Lin, H. X. Jiang, C. M. Sorensen, Applied Physics Letters 67 (1995) 81.
[7] O. Z. Angel, A. E. E. Garcia, C. Falcony, R. L. Morales, R. R. Bon, Solid State Communications 94 (1995) 81.
[8] H.S. Nalwa, 'Nanostructured materials and nanotechnology, (concise edn.)', Academic Press, San Diego, 2002.
[9] J.R. Heath, Science 270 (1995) 1315.
[10] C.B. Murray, C.R. Kagan, M.G. Bawendi, Science 270 (1995) 1335.
[11] D.U. Wiechert et al. / Thin Solid Films 484 (2005) 73.
[12] B.D. Cullity, 'Elements of X-ray diffraction (2^{nd} edn.)', Addison Wesley, New York, 1978.
[13] C.K. Mahadevan, Physica B, 403 (2008) 57.
[14] M. Meena and C.K. Mahadevan, Cryst. Res. Technol. 43 (2008) 166.
[15] M. Priya and C.K. Mahadevan, Physica B, 403 (2008) 67.
[16] Rajeswari Yogamalar, Ramasamy Srinivasan, Ajayan Vinu, Katsuhiko Ariga, Arumugam Chandra Bose, Solid State Communications, 149 (2009)1919.
[17] S.V. Gaponenko, 'Optical Properties of Semiconductor Nanocrystals', Cambridge University Press, Cambridge, 1998.
[18] C. Kittel, 'Introduction to Solid State Physics (7^{th} Edn.)', Wiley Eastern Limited, New Delhi, 1996.